

# A Reaction Between High Mn-High Al Steel and CaO-SiO<sub>2</sub>-Type Molten Mold Flux: Part I. Composition Evolution in Molten Mold Flux

MIN-SU KIM, SU-WAN LEE, JUNG-WOOK CHO, MIN-SEOK PARK,  
HAE-GEON LEE, and YOUN-BAE KANG

In order to elucidate the reaction mechanism between high Mn-high Al steel such as twin-induced plasticity steel and molten mold flux composed mainly of CaO-SiO<sub>2</sub> during continuous casting process, a series of laboratory-scale experiments were carried out in the present study. Molten steel and molten flux were brought to react in a refractory crucible in a temperature range between 1713 K to 1823 K (1440 °C to 1550 °C) and composition evolution in the steel and the flux was analyzed using inductively coupled plasma atomic emission spectroscopy, X-ray fluorescence, and electron probe microanalysis. The amount of SiO<sub>2</sub> in the flux was significantly reduced by Al in the steel; thus, Al<sub>2</sub>O<sub>3</sub> was accumulated in the flux as a result of a chemical reaction,  $4[\text{Al}] + 3(\text{SiO}_2) = 3[\text{Si}] + 2(\text{Al}_2\text{O}_3)$ . In order to find a major factor which governs the reaction, a number of factors ((pct CaO/pct SiO<sub>2</sub>), (pct Al<sub>2</sub>O<sub>3</sub>), [pct Al], [pct Si], and temperature) were varied in the experiments. It was found that the above chemical reaction was mostly governed by [pct Al] in the molten steel. Temperature had a mild effect on the reaction. On the other hand, (pct CaO/pct SiO<sub>2</sub>), (pct Al<sub>2</sub>O<sub>3</sub>), and [pct Si] did not show any noticeable effect on the reaction. Apart from the above reaction, the following reactions are also thought to happen simultaneously:  $2[\text{Mn}] + (\text{SiO}_2) = [\text{Si}] + 2(\text{MnO})$  and  $2[\text{Fe}] + (\text{SiO}_2) = [\text{Si}] + 2(\text{FeO})$ . These oxide components were subsequently reduced by Al in the molten steel. Na<sub>2</sub>O in the molten flux was gradually decreased and the decrease was accelerated by increasing [pct Al] and temperature. Possible reactions affecting the Al<sub>2</sub>O<sub>3</sub> accumulation are summarized.

DOI: 10.1007/s11663-012-9770-z

© The Minerals, Metals & Materials Society and ASM International 2012

## I. INTRODUCTION

RECENT advances in the development of high-alloyed steel such as twin-induced plasticity (TWIP) steel have been led by noticeable product performance such as its extraordinary ductility and high tensile strength. Thanks to its high strain-hardening rate associated with dynamic strain aging and mechanical twins, the TWIP steel has attracted much attention as a next-generation automotive steel.<sup>[1]</sup> In the TWIP steel, the addition of Al is a usual practice because it is indispensable to suppress delayed fractures in the press-formed parts of the TWIP steel.<sup>[2,3]</sup> Moreover, the

addition of Al also increases the stacking fault energy which is linked to the deformation mechanism<sup>[4]</sup> such that increasing the stacking fault energy changes the deformation mode from  $\epsilon$ -martensite formation to mechanical twinning during the deformation of austenite. High Al content in the steel also additionally reduces weight of the steel, which is favorable in reducing automobile weight.

However, contrary to those beneficial aspects on the product side, such high Al content in the steel induces severe process difficulties such as poor casting performances. In particular, among a number of issues responsible for the poor casting performances, strong chemical reactions taking place at the interface between molten steel and molten mold flux during the continuous casting process cause several operating problems. The problems stem from Al<sub>2</sub>O<sub>3</sub> accumulation (coupled with SiO<sub>2</sub> reduction) in the mold flux. This significantly affects the physico-chemical properties of the flux (viscosity, melting behavior, crystallization, heat transfer, *etc.*).

A continuous casting process for a similar kind of high Al steel such as transformation-induced plasticity (TRIP) steel suffers problems such as breakout prediction (BOP) alarms, poor surface quality (transverse and longitudinal depressions), sticking on hot slabs, and deterioration of conditions in the mold.<sup>[5,6]</sup> A casting of a nonmagnetic high Mn-high Al steel (21 to 25 Mn-1.5 to 2.5 Al) also suffers similar problems.<sup>[7,8]</sup> In order to

---

MIN-SU KIM, Graduate Student, HAE-GEON LEE, Professor Emeritus, and YOUN-BAE KANG, Assistant Professor, are with the Graduate Institute of Ferrous Technology, Pohang University of Science and Technology, Pohang 790-784, Republic of Korea. Contact e-mail: ybkang@postech.ac.kr SU-WAN LEE, formerly Graduate Student with the Graduate Institute of Ferrous Technology, Pohang University of Science and Technology, is now Engineer with the Steelmaking Department, Pohang Works, POSCO Ltd, Pohang, Republic of Korea. JUNG-WOOK CHO, formerly Principal Researcher with the Technical Research Laboratories, POSCO Ltd, Gwangyang, Republic of Korea, is now Research Associate Professor with the Graduate Institute of Ferrous Technology, Pohang University of Science and Technology. MIN-SEOK PARK, Senior Researcher, is with the Technical Research Laboratories, POSCO Ltd.

Manuscript submitted August 21, 2012.

Article published online December 11, 2012.

avoid such problems, POSCO Gwangyang works has tried to supply “molten mold flux” directly into the casting mold during continuous casting of their TWIP steel production.<sup>[9]</sup> Nevertheless, the strong chemical reaction still persists, thus resulting in Al<sub>2</sub>O<sub>3</sub> accumulation in the molten mold flux.

There have been a number of investigations on this issue, but those investigations were conducted in industry, thus mainly focusing on development of new mold flux (CaO-Al<sub>2</sub>O<sub>3</sub> type) which seems inert to Al in molten steel.<sup>[5,6]</sup> Although the CaO-Al<sub>2</sub>O<sub>3</sub>-type flux has shown some promising results that the degree of steel/flux interaction could be minimized, it exhibits other problems such as increased viscosity and reduced consumption, thereby resulting in inadequate lubrication.<sup>[5]</sup> On the other hand, fundamental research on the chemical interactions between molten high-alloyed steel and molten mold flux (conventional CaO-SiO<sub>2</sub> type) is very scarce. Yu *et al.*<sup>[7]</sup> and Wang *et al.*<sup>[8]</sup> have investigated the behavior of CaO-SiO<sub>2</sub>-type mold flux during continuous casting of high Mn-high Al nonmagnetic steel (21 to 25 Mn-1.5 to 2.5 Al). In their casting practice, Wang *et al.*<sup>[8]</sup> observed a significant Al<sub>2</sub>O<sub>3</sub> accumulation, as much as 25 pct in 2000 seconds (over 30 minutes). Yu *et al.*<sup>[7]</sup> and Wang *et al.*<sup>[8]</sup> developed model equations to predict the Al<sub>2</sub>O<sub>3</sub> accumulation in the mold flux based on a dynamic mass balance. However, they assumed that the Al<sub>2</sub>O<sub>3</sub> accumulation is rate controlled by Al<sub>2</sub>O<sub>3</sub> mass transfer in the mold flux phase, which has never been confirmed. Although it is clear that the conventional CaO-SiO<sub>2</sub>-type mold flux is not adequate to be directly used in the casting of the high Mn-high Al steel such as TWIP steel, it is still necessary to elucidate a reaction mechanism between the conventional CaO-SiO<sub>2</sub>-type molten mold flux and the high Mn-high Al steel in order to guide the development of new mold flux which retards the Al<sub>2</sub>O<sub>3</sub> accumulation.

Therefore, in the present study, elucidation of the reaction mechanism between the conventional CaO-SiO<sub>2</sub>-type mold flux (CaO-SiO<sub>2</sub>-Al<sub>2</sub>O<sub>3</sub>-MgO-Na<sub>2</sub>O-F) and the high Mn-high Al steel (Fe-C-Mn-Al-Si) by seeking a major factor affecting the Al<sub>2</sub>O<sub>3</sub> accumulation in the mold flux has been attempted. A series of steel/flux reaction experiments were carried out, followed by kinetic analysis. Interfacial morphology was also taken into account to propose a reaction mechanism. The proposed reaction mechanism was then utilized to develop a model equation to predict Al<sub>2</sub>O<sub>3</sub> concentration in the molten mold flux during the continuous casting process.

The results obtained in the present study are reported in a series of two articles. The present article, which is a first of the present series, is composed as follows. A brief literature survey is reported in order to summarize previous knowledge on the slag/steel interfacial reaction in the view of reaction mechanism and interfacial morphology, focusing on a reaction between Al and SiO<sub>2</sub>. Details of the laboratory-scale experiment including choice of refractory crucibles are then shown. Composition evolutions in molten mold flux/molten steel are followed, and the manner in which those composition evolutions are affected by various factors

including (pct CaO/pct SiO<sub>2</sub>), (pct Al<sub>2</sub>O<sub>3</sub>), [pct Al], [pct Si], and temperature will be shown. Several reactions taking place at the interface are summarized. Comprehensive discussions about kinetic analysis, and the reaction mechanism, and a model development will be continued in the second article in the present series.<sup>[10]</sup>

## II. LITERATURE SURVEY

In this section, relevant literature information is collected and summarized in order to understand up-to-date advances on the slag-metal interfacial reaction, in particular for reduction of weak oxide components by active solutes in liquid steel.

### A. Reduction of Oxide Components by Solutes in Liquid Steel

One of the most extensive investigations on this kind of topic is the reduction of SiO<sub>2</sub> in molten slag by C in liquid iron.<sup>[11–16]</sup> The practical importance of the reduction of SiO<sub>2</sub> by C is due to the control of Si level in hot metal produced in a blast furnace. Most of the previous investigations have agreed that the reduction of SiO<sub>2</sub> by C is very sluggish: (SiO<sub>2</sub>) + 2[C] = [Si] + 2CO(g). They concluded that the rate of the reduction of SiO<sub>2</sub> is controlled by a chemical reaction at the interface between the slag and the liquid iron. Reported values of activation energy for the reaction are generally high: 544 kJ/mol,<sup>[11]</sup> 370 to 420 kJ/mol,<sup>[14]</sup> 840 kJ/mol,<sup>[13]</sup> 238 kJ/mol,<sup>[16]</sup> 280 to 405 kJ/mol.<sup>[15]</sup> Most of these values fall in the range of a chemical reaction control.<sup>[13]</sup> In particular, Fulton and Chipman proposed that the slowest step would be a breaking of Si-O bond in the slag phase, which requires a high activation energy. Although some investigators reported a somewhat different rate-controlling step (mass transport of O in liquid iron below 1873 K (1600 °C),<sup>[13]</sup> mixed control between chemical reaction at the interface and mass transport in slag phase<sup>[14]</sup>), the overall rate of the reduction of SiO<sub>2</sub> seems to be governed by the chemical reaction.<sup>[11,12,15,16]</sup> Turkdogan *et al.*<sup>[12]</sup> attributed this to the limited site for the reaction which involves three phases: slag, liquid iron, and gas phase.

On the other hand, a reaction mechanism of SiO<sub>2</sub> reduction by Al in liquid iron has not yet been clarified. Although Riboud and co-workers<sup>[17,18]</sup> investigated the reaction between SiO<sub>2</sub> in slag and Al in liquid iron drop in the slag (3(SiO<sub>2</sub>) + 4[Al] = 2(Al<sub>2</sub>O<sub>3</sub>) + 3[Si]), those investigations focused mainly on determination of interfacial tension between the two phases and emulsification of the liquid iron phase into the slag. In those investigations, it was observed that apparent interfacial tension decreased rapidly to almost zero. This implies that there was very intense chemical reaction at the interface between the slag and the liquid iron. According to their chemical analysis, [pct Al] in the liquid iron phase during the reaction decreased linearly with time. This implies that the presence of Al in the liquid iron did not participate in the rate equation for the SiO<sub>2</sub> reduction (consequently, the Al<sub>2</sub>O<sub>3</sub> accumulation). This

is in agreement with an earlier report by Ooi *et al.*<sup>[19]</sup> In their investigation (reaction between 40CaO-40SiO<sub>2</sub>-20Al<sub>2</sub>O<sub>3</sub> slag and Fe-4Al in mass pct.), they concluded that the rate-controlling step for the above reaction was the chemical reaction at the interface between the slag and the liquid iron. However, their investigation<sup>[19]</sup> relied on only two experimental data points.

Ozturk and Turkdogan<sup>[20]</sup> and Sun and Mori<sup>[21]</sup> suggested that if SiO<sub>2</sub> concentration in slag is less than 5 to 10 mass pct, the above reaction rate would be slow. Ozturk and Turkdogan<sup>[20]</sup> further discussed that the activity of the SiO<sub>2</sub> in such low-SiO<sub>2</sub> slag was in the range of 10<sup>-5</sup> to 10<sup>-4</sup>, which lowers driving force for the above reaction. However, it is not clear that whether low activity of SiO<sub>2</sub> or slow mass transfer of the SiO<sub>2</sub> to the reaction interface is responsible for the slow reaction rate.

Rhamdhani *et al.*<sup>[22]</sup> investigated reaction kinetics between 40CaO-40SiO<sub>2</sub>-20Al<sub>2</sub>O<sub>3</sub> slag and Fe-Al alloy ([pct Al] = 3.5 to 5). They observed an exponential decay of [pct Al], which was different from the earlier observations.<sup>[17-19]</sup> From a kinetic analysis, they concluded that rate of the above reaction was controlled by mass transfer of Al in the liquid Fe-Al alloy, and the mass transfer coefficient of Al ( $k_{Al}$ ) was 1.3 to  $1.9 \times 10^{-6}$  m/s in the temperature range of 1823 K to 1923 K (1550 °C to 1650 °C). From an Arrhenius-type plot of the mass transfer coefficients, they obtained the activation energy of 127 kJ/mol for the mass transfer. This is close to the category of mass transfer control in the metal phase.<sup>[23]</sup> The measured mass transfer coefficient is one order lower than the value reported by Forster and Richter<sup>[24]</sup> ( $1.2 \times 10^{-5}$  m/s).

Still, it is not clear whether the reaction kinetics between molten steel and molten flux is controlled by mass transport or chemical reaction at the interface. Therefore, it would be very desirable if thermodynamic activity data of components involving the reaction are available. In particular, activities of SiO<sub>2</sub> in the flux would be useful indicators of whether the SiO<sub>2</sub> would be reduced or not. As Ozturk and Turkdogan reported,<sup>[20]</sup> the activity of SiO<sub>2</sub> in the range of 10<sup>-5</sup> to 10<sup>-4</sup> lowers the driving force of the SiO<sub>2</sub> reduction. However, such activity data in a practical mold flux system are very scarce.

### B. Interfacial Instability Between Molten Steel and Molten Slag

There have been a number of investigations on interfacial instability between molten steel and molten slag.<sup>[17,19,25-29]</sup> Many of these investigations focused on fragmentation of molten metal into many numbers of droplets in order to enlarge the reaction interface. Such metal droplets were emulsified in the molten slag phase, and due to a large increase of the reaction interface, a very rapid reaction rate could be obtained.<sup>[25]</sup> Most of these investigations involved CO gas generation which accelerated the droplet formation. On the other hand, without C in steel, some researchers found that small droplets could be generated from the reaction interface between molten steel and molten slag, or the reaction

interface could become very irregular.<sup>[17,18,22,27,29,30]</sup> Riboud and Lucas<sup>[17]</sup> and Gaye *et al.*<sup>[18]</sup> attributed such irregularity and fragmentation into small droplets to the fact that intense mass transfer through the interface decreased the interfacial tension (even close to zero for the reaction between Fe-4.45 pct Al + CaO-Al<sub>2</sub>O<sub>3</sub>-SiO<sub>2</sub> slag). By using X-ray photography, Chung and Cramb<sup>[27,29]</sup> observed a “dynamic interfacial phenomena” of a metal droplet in molten slag, which consisted of droplet flattening, interfacial turbulence, spontaneous emulsification, and reconstruction of the original droplet. This observation is practically very important in the light of enhancement of the reaction rate enormously. Rhamdhani *et al.*<sup>[22]</sup> attempted to take into account such instantaneous increase of reaction interfacial area in their kinetic analysis.

However, in these investigations, possible retardation of the reaction by formation of saturated solid phase in the slag phase was not considered. Kim and Park<sup>[30]</sup> observed a significant retardation of the reaction between molten steel (Fe-Mn-Al) and molten slag (CaO-SiO<sub>2</sub>-Al<sub>2</sub>O<sub>3</sub>-MgO), and such a tendency was more significant as initial [pct Al] in the liquid steel was high. They observed several solid oxide phases formed near the reaction interface between the molten steel and the molten slag. They attributed such delay of the reaction to the fact that increasing viscosity in the solid-saturated slag slowed down the transportation of reactants and products near the reaction interface.

From the above literature survey, it is concluded that the reaction rate between Al in molten steel and SiO<sub>2</sub> in molten slag is necessary to be evaluated based on a clearly evidenced reaction mechanism. Furthermore, careful examination at the interface is necessary because formation of solid phase as a reaction product would alter the reaction mechanism, which in turn could change the reaction rate.

## III. EXPERIMENTAL

In order to investigate the reaction kinetics and the reaction mechanism between molten flux and molten steel, a laboratory-scale experiment was carried out in the present study. In general, the molten flux and the molten steel were brought in contact in a refractory crucible to begin chemical reactions at the interface. Samples of the flux and the steel were taken periodically and their compositions were analyzed. In some cases, a concentration profile in the molten flux was examined using an electron microprobe. Compositions reported in the present paper are all in mass pct.

### A. Reaction Kinetics

A schematic figure of the experimental equipment used in the present study is shown in Figure 1. About 400 g of steel sample was charged in a refractory crucible made of MgO (OD 60 mm × ID 52 mm × H 100 mm). The steel sample in the crucible was melted in a reaction chamber made of a quartz tube equipped with water-cooled brass end caps in an induction furnace. The

temperature of the furnace was controlled by a PID (Proportional-Integral-Derivative) controller connected to a B-type thermocouple placed at the bottom of the crucible. The reaction temperature was set at a desired temperature between 1713 K and 1823 K (1440 °C and 1550 °C). Ar gas purified by passing through silica gel and Mg chips heated at 723 K (450 °C) was flown in the reaction chamber through the experiment. After the steel was fully melted, a Fe boat filled with pre-fused and ground flux powder as much as 44 g was brought to the molten steel. The Fe boat was lowered to contact with the molten steel in order for the flux to flow out of the boat. The flux melts on the molten steel and this

moment was set as zero time. Using quartz tubes, the steel and the flux samples were taken periodically up to 20 minutes and were rapidly quenched into ice water. Concentrations of Mn, Si, and Al in the steel samples were analyzed by inductively coupled plasma atomic emission spectroscopy (ICP-AES), while those of CaO, SiO<sub>2</sub>, Al<sub>2</sub>O<sub>3</sub>, MgO, Na<sub>2</sub>O, and F in the flux samples were analyzed by X-ray fluorescence (XRF). Initial compositions of steel and flux samples used in the present study are shown in Table I.

### B. Crucible Selection

One of the difficulties encountered in the present study was an erosion of a refractory crucible by the molten flux. In preliminary tests, four different kinds of refractory crucibles were employed in order to evaluate their applicability in the present experiment. The kinds of the refractory crucibles were (1) MgO, (2) Al<sub>2</sub>O<sub>3</sub>, (3) ZrO<sub>2</sub>, and (4) MgAl<sub>2</sub>O<sub>4</sub> crucibles. In each crucible, a steel sample (S1) was melted, and a molten flux (F1) was poured onto the steel melt, as described in the previous section. Compositions of the flux samples were chemically analyzed as described in the previous section.

### C. Composition Profile in Flux

In order to observe composition homogeneity in the molten flux, a similar experiment was carried out in a resistance furnace, but smaller MgO crucibles (OD 18 mm × ID 15 mm × H 50 mm) were employed. One minute after the reaction between the liquid steel (S1) and the molten flux (F3), the crucibles were rapidly quenched in ice water. The crucible with the steel/flux was mounted with an epoxy resin, cut perpendicular to the reaction interface, and then observed by an electron microscope. The composition profile of flux components was analyzed using electron probe microanalysis (EPMA).

- A. Mo wire
- B. Gas outlet
- C. Fe boat filled with slag
- D. Alumina protection tube
- E. Refractory crucible
- F. Steel
- G. Graphite susceptor
- H. Gas inlet
- I. Pt-30Rh/Pt-6Rh thermocouple
- J. Water-cooled brass end-cap
- K. Alumina pedestal
- L. Induction coil
- M. Quartz tube
- N. Quartz sampling tube

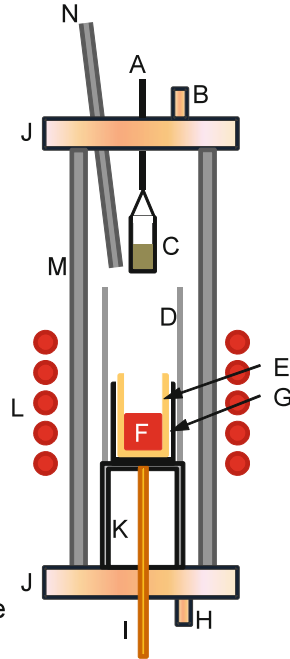


Fig. 1—Experimental equipment employed in the present study.

Table I. Initial Compositions of Steel and Flux Samples Used in the Present Study (Mass Percent)

No.	Steel						Note
	Fe	C	Al	Si	Mn		
S1	bal.	0.65	1.77	0.70	13.2	reference	
S2	bal.	0.65	0.41	0.72	13.1	0.4 Al	
S3	bal.	0.65	0.92	0.69	13.1	0.9 Al	
S4	bal.	0.65	4.77	0.65	13.1	4.8 Al	
S5	bal.	0.65	1.61	0.11	12.8	0.1 Si	
S6	bal.	0.65	1.60	0.42	13.1	0.4 Si	
S7	bal.	0.65	1.66	1.66	12.8	1.7 Si	

No.	Flux						Note
	CaO	SiO <sub>2</sub>	Al <sub>2</sub> O <sub>3</sub>	MgO	Na <sub>2</sub> O	F	
F1	36.53	33.63	5.82	2.54	13.81	7.66	reference
F2	16.90	53.47	5.67	2.49	13.81	7.66	0.3 CaO/SiO <sub>2</sub>
F3	26.69	43.73	5.76	2.35	13.81	7.66	0.6 CaO/SiO <sub>2</sub>
F4	38.97	36.65	0.00	2.90	13.81	7.66	0 Al <sub>2</sub> O <sub>3</sub>
F5	34.07	31.36	12.16	2.37	12.88	7.15	12 Al <sub>2</sub> O <sub>3</sub>

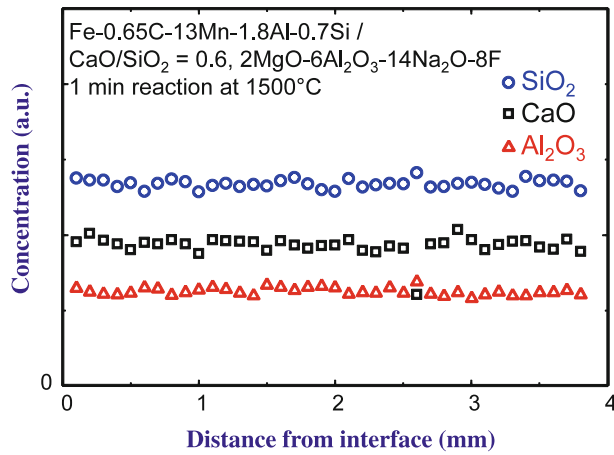


Fig. 2—Composition homogeneity in molten flux (F3) reacted with molten steel (S1) for 1 min at 1773 K (1500 °C). Concentrations are only semi-quantitative.

#### IV. RESULTS AND DISCUSSION

In the present study, composition evolutions of steel/flux samples for various experimental conditions were obtained. By reacting steel and flux samples shown in Table I at 1773 K (1500 °C), the effect of various factors ((pct CaO/pct SiO<sub>2</sub>), (pct Al<sub>2</sub>O<sub>3</sub>), [pct Al], and [pct Si]) on the reaction was examined. Also, additional experiments were carried out at different temperatures in order to examine the effect of temperature on the reaction. Before the actual experiments were performed, applicability of various refractory crucibles was also tested.

##### A. Choice of Refractory Crucible

While chemical reactions mainly take place at the interface between molten steel and molten flux, an additional reaction also takes place between the flux and the crucible. By the chemical analysis of flux samples periodically taken during the reaction up to 10 minutes, the applicability of the crucibles in the present study was examined. In the case of the MgO crucible, the concentration of MgO increased as much as 3 to 4 mass pct for 10 minutes of reaction. In the case of the Al<sub>2</sub>O<sub>3</sub> crucible, the concentration of Al<sub>2</sub>O<sub>3</sub> increased not only by the reaction between the flux and the crucible, but also by other reactions between the flux and the steel. Compared to the MgO crucible case where only the reaction between the flux and the steel contributed to the increase of the Al<sub>2</sub>O<sub>3</sub> concentration, the concentration of Al<sub>2</sub>O<sub>3</sub> in the Al<sub>2</sub>O<sub>3</sub> crucible increased 3 to 4 mass pct more than that in the MgO crucible for 10 minutes of reaction. It seems that Al<sub>2</sub>O<sub>3</sub> erosion from the Al<sub>2</sub>O<sub>3</sub> crucible was as much as 3 to 4 mass pct in the 10 minutes. In the case of the ZrO<sub>2</sub> crucible, ZrO<sub>2</sub> concentration was about 3 mass pct after the 10 minutes of reaction. On the other hand, the MgAl<sub>2</sub>O<sub>4</sub> crucible was eroded significantly. Therefore, the MgAl<sub>2</sub>O<sub>4</sub> crucible could not be used. For the purpose of the present study, the observation of Al<sub>2</sub>O<sub>3</sub> concentration in molten flux is one of the major points. Therefore, the Al<sub>2</sub>O<sub>3</sub>

crucible was not considered anymore. Chemical stability of the ZrO<sub>2</sub> crucible was fine, but it was weak to a thermal shock. Therefore, in the present study, the MgO crucible was finally chosen for further experiments.

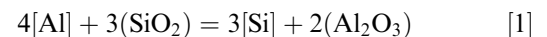
##### B. General Composition Evolution: Homogeneity and Time Evolution

In the present study, it was assumed that the analyzed compositions of the steel and the flux obtained by the quartz tube represented bulk compositions of the steel and the flux. This implies that the two phases were assumed to be almost homogeneous outside the boundary layers. In the case of the steel phase, the assumption seems reasonable because a strong agitation by the induction furnace was applied to the steel phase. In the case of the molten flux, in order to check the homogeneity, a composition analysis in the quenched flux sample (F3) reacted with steel (S1) was carried out as described in Section III-C. Since Na and F are very difficult to analyze quantitatively using the EPMA, only a semi-quantitative analysis was carried out, and thus no absolute scale of the concentrations is shown in the figure. As shown in Figure 2, concentration profiles over the flux sample from steel/flux interface to bulk flux do not vary significantly. As the flux contains Na and F which typically increase fluidity of the flux, it is considered that the flux (outside boundary layer) was homogeneous during the experiment. Therefore, the samples taken by a quartz tube during the experiments were assumed to represent bulk of the flux at each moment.

Figure 3 shows composition evolution during the reaction between steel (S1) and flux (F1) at 1773 K (1500 °C) as time passes as an example of all other runs. As expected, (pct Al<sub>2</sub>O<sub>3</sub>) increased, while (pct SiO<sub>2</sub>) decreased as seen in the Figure 3(a). At the same time, [pct Al] decreased, while [pct Si] increased as seen in the Figure 3(b). Such composition evolution was observed in all runs in the present study. (pct MgO) gradually increased and this was attributed to the erosion of the crucible as mentioned in the Section IV-A. For the volatile components such as Na and F, (pct Na<sub>2</sub>O) kept decreasing as much as 5 mass pct for 10 minutes, while F did not show any noticeable change. (pct Fe<sub>2</sub>O) and (pct MnO) which were zero at the beginning of the reaction slightly increased to a few mass pct. Due to the large mass ratio of steel/flux and small increase of (pct MnO), [pct Mn] did not vary noticeably.

From the above observation, it is found that:

- (1) The most significant reaction taking place at the interface between the molten steel and the molten flux is



- (2) Na<sub>2</sub>O in the flux gradually disappears and it may be attributed to the vaporization of the Na<sub>2</sub>O or reduction of Na<sub>2</sub>O to [Na].
- (3) (pct F) in the flux does not vary significantly.

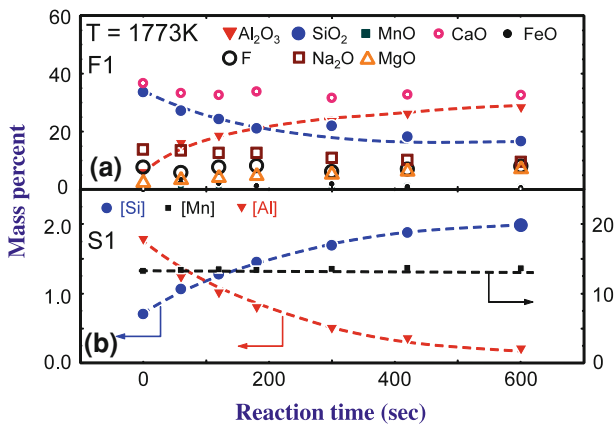


Fig. 3—Composition evolution in molten flux (F1) and molten steel (S1) reacted at 1773 K (1500 °C): (a) molten flux and (b) molten steel.

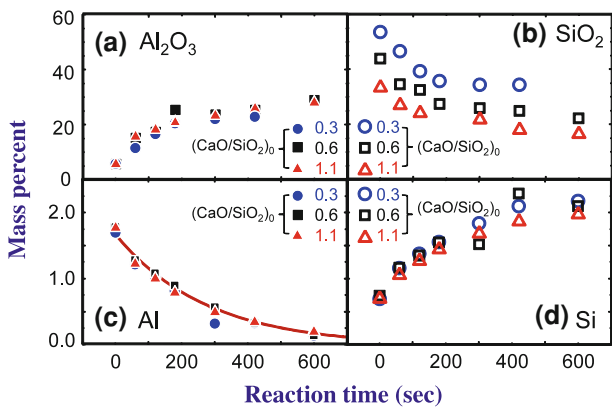


Fig. 4—Effect of (pct CaO)/(pct SiO<sub>2</sub>) on the composition evolution in molten flux (F1, F2, and F3) and molten steel (S1) reacted at 1773 K (1500 °C): (a) (pct Al<sub>2</sub>O<sub>3</sub>), (b) (pct SiO<sub>2</sub>), (c) [pct Al], and (d) [pct Si]. Line in (c) is a calculated [pct Al] using a kinetic equation described in the second article in the present series.<sup>[10]</sup>

(4) Fe<sub>2</sub>O and MnO increase during the reaction, but the extent of the increase was not significant.

Among the above four observations, Reaction [1] affects most significantly the physical properties of the molten flux and consequently the casting performance. Therefore, in the present study, the observation and discussion are mainly focused on Reaction [1].

Among variables which may affect the accumulation of Al<sub>2</sub>O<sub>3</sub> as well as the reduction of SiO<sub>2</sub> in molten flux, in the present study, (pct CaO/pct SiO<sub>2</sub>), (pct Al<sub>2</sub>O<sub>3</sub>), [pct Al], temperature, and [pct Si] were considered. In the following sections, the effect of such variables on Reaction [1] is shown by the experimental data obtained in the present study.

It should be noted that the concentration evolution reported in the present article represents concentration in the steel contained in a crucible. Therefore, [pct Al] decreased quickly to a very low level. On the other hand, actual concentrations observed in casted steel after the continuous casting process will be different, as the casting process is an open system.

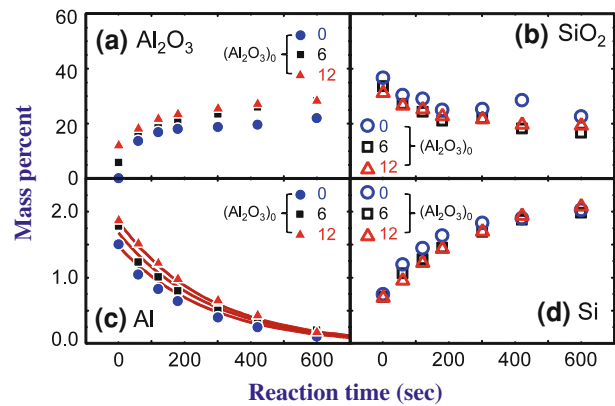


Fig. 5—Effect of (pct Al<sub>2</sub>O<sub>3</sub>) on the composition evolution in molten flux (F1, F4, and F5) and molten steel (S1) reacted at 1773 K (1500 °C): (a) (pct Al<sub>2</sub>O<sub>3</sub>), (b) (pct SiO<sub>2</sub>), (c) [pct Al], and (d) [pct Si]. Lines in (c) are calculated [pct Al] using a kinetic equation described in the second article in the present series.<sup>[10]</sup>

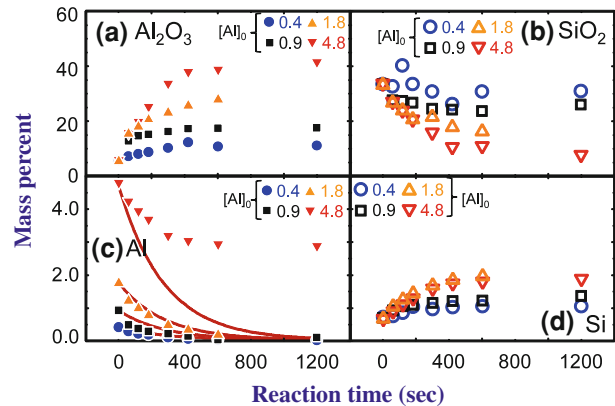


Fig. 6—Effect of [pct Al] on the composition evolution in molten flux (F1) and molten steel (S1, S2, S3, and S4) reacted at 1773 K (1500 °C): (a) (pct Al<sub>2</sub>O<sub>3</sub>), (b) (pct SiO<sub>2</sub>), (c) [pct Al], and (d) [pct Si]. Lines in (c) are calculated [pct Al] using a kinetic equation described in the second article in the present series.<sup>[10]</sup>

### C. Effect of Various Factors on Steel/Flux Reaction: (pct Al<sub>2</sub>O<sub>3</sub>), (pct SiO<sub>2</sub>), [pct Al], Temperature, and [pct Si]

In this section, experimentally obtained compositions of components in mold flux and molten steel are presented. By observing the composition evolutions, the major factor(s) affecting the Al<sub>2</sub>O<sub>3</sub> accumulation are revealed. As Reaction [1] is shown to be most dominant at the interface, concentrations of Al<sub>2</sub>O<sub>3</sub> and SiO<sub>2</sub> in molten flux and those of Al and Si in molten steel are shown. Those experimental data measured in the present study are shown as symbols in Figures 4 through 8. Solid lines shown for [pct Al] in those figures are calculated concentrations of Al in molten steel by a kinetic equation developed in the second article in the present series, which will be discussed in the second article.<sup>[10]</sup>

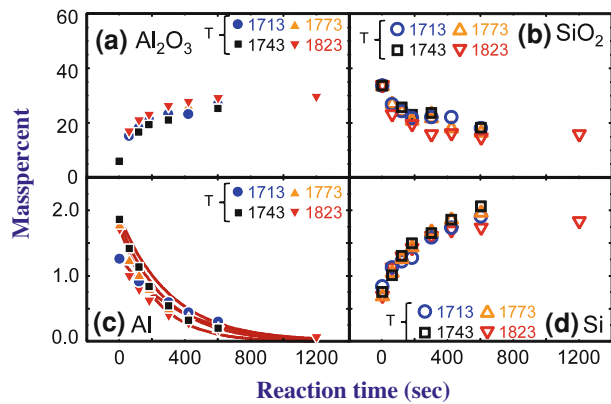


Fig. 7—Effect of reaction temperature on the composition evolution in molten flux (F1) and molten steel (S1) reacted at 1713 K to 1823 K (1440 °C to 1550 °C): (a) (pct Al<sub>2</sub>O<sub>3</sub>), (b) (pct SiO<sub>2</sub>), (c) [pct Al], and (d) [pct Si]. Lines in (c) are calculated [pct Al] using a kinetic equation described in the second article in the present series.<sup>[10]</sup>

### 1. Effect of (pct CaO)/(pct SiO<sub>2</sub>) in molten flux

As SiO<sub>2</sub> in mold flux is a major weak oxide to be reduced, availability of SiO<sub>2</sub> in the flux may affect the rate of Al<sub>2</sub>O<sub>3</sub> accumulation in the flux. Figure 4 shows the evolution of compositions of SiO<sub>2</sub> and Al<sub>2</sub>O<sub>3</sub> in the molten flux and those of Si and Al in the liquid steel, when the initial (pct CaO)/(pct SiO<sub>2</sub>) in the molten fluxes were different (0.3, 0.6, and 1.1). Similar to the result shown in Figure 3, (pct Al<sub>2</sub>O<sub>3</sub>) rapidly increased from 6 to 30 within 10 minutes, while (pct SiO<sub>2</sub>) rapidly decreases. The extent of the SiO<sub>2</sub> reduction looks less sensitive to the (pct CaO)/(pct SiO<sub>2</sub>) and the rate of Al<sub>2</sub>O<sub>3</sub> accumulation looks almost similar to each other. At the same time, Si in the molten steel increased accordingly, but the rate of Si increase in the molten steel is irrelevant to the (pct CaO)/(pct SiO<sub>2</sub>). Similarly, Al in the liquid steel decreased, but the rate of the Al decrease in the molten steel is irrelevant to the (pct CaO)/(pct SiO<sub>2</sub>) too. These observations imply that Reaction [1] took place and it was not considerably affected by the (pct CaO)/(pct SiO<sub>2</sub>) in the molten flux. Therefore, the (pct CaO)/(pct SiO<sub>2</sub>) is not a critical factor for the control of Al<sub>2</sub>O<sub>3</sub> accumulation in the present study.

### 2. Effect of initial (pct Al<sub>2</sub>O<sub>3</sub>) in molten flux

Since Al<sub>2</sub>O<sub>3</sub> is a product of Reaction [1], a high concentration of Al<sub>2</sub>O<sub>3</sub> in molten flux may retard the reaction rate of Al<sub>2</sub>O<sub>3</sub> accumulation and SiO<sub>2</sub> reduction if a backward reaction of Reaction [1] is considerable. Figure 5 shows the evolution of compositions of SiO<sub>2</sub> and Al<sub>2</sub>O<sub>3</sub> in the molten flux and those of Si and Al in the molten steel when the initial (pct Al<sub>2</sub>O<sub>3</sub>) in molten fluxes were different (0, 6, and 12). Similar to the observation in the previous section, reduction of the SiO<sub>2</sub> and accumulation of the Al<sub>2</sub>O<sub>3</sub> were not noticeably affected by the initial (pct Al<sub>2</sub>O<sub>3</sub>). This is more evident by the observation of increase of [pct Si] and decrease of [pct Al] that the tendency of [pct Si] increase and that of [pct Al] decrease are almost identical, irrespective of the initial (pct Al<sub>2</sub>O<sub>3</sub>). Therefore, the initial (pct Al<sub>2</sub>O<sub>3</sub>) is

not a critical factor for the control of Al<sub>2</sub>O<sub>3</sub> accumulation in the present study.

### 3. Effect of initial [pct Al] in steel

Because Al in molten steel is one of the most likely components to reduce SiO<sub>2</sub> in molten flux, the effect of different initial [pct Al] (0.4, 0.9, 1.8, and 4.8) was examined in the present study and the result is shown in Figure 6. The rate of Al<sub>2</sub>O<sub>3</sub> accumulation and that of SiO<sub>2</sub> reduction are seen to be strongly affected by initial [pct Al] and this observation is different from those in the previous sections. As the initial [pct Al] increased, the rate of Al<sub>2</sub>O<sub>3</sub> accumulation and that of SiO<sub>2</sub> reduction were accelerated, although some scatters were seen for the (pct SiO<sub>2</sub>). Such phenomena are seen more clearly by the change of [pct Si] that the higher the initial [pct Al], the more the [pct Si] increases through Reaction [1]. Therefore, the initial [pct Al] is a critical factor for the control of Al<sub>2</sub>O<sub>3</sub> accumulation in the present study.

### 4. Effect of temperature

As Reaction [1] takes place by breaking the Si-O network of SiO<sub>2</sub> and forming Al<sub>2</sub>O<sub>3</sub> in molten flux, the rate of the reaction is likely to be dependent on temperature. Figure 7 shows the result of the present experiment under different temperatures from 1713 K to 1823 K (1440 °C to 1550 °C). Compared to the result shown in the Section IV-C-3, the temperature affected less significantly the composition changes than the initial [pct Al] did. Nevertheless, there is noticeable effect of temperature in such a way that the rate of Al<sub>2</sub>O<sub>3</sub> accumulation increases as temperature increases. Therefore, temperature is also a considerable factor for the control of Al<sub>2</sub>O<sub>3</sub> accumulation in the present study.

### 5. Effect of initial [Si] in steel

Increasing Si content in molten steel may also affect the rate of SiO<sub>2</sub> reduction and Al<sub>2</sub>O<sub>3</sub> accumulation, if a backward reaction of Reaction [1] is considerable. In the present study, molten steels with different initial [pct Si] were brought to react with molten fluxes, and the corresponding composition changes in the molten steel and the molten flux are shown in Figure 8. As seen in the figure, a decrease of (pct SiO<sub>2</sub>), increase of (pct Al<sub>2</sub>O<sub>3</sub>), and decrease of [pct Al] are all irrespective of the initial [pct Si]. Therefore, the initial [pct Si] is not a critical factor for the control of Al<sub>2</sub>O<sub>3</sub> accumulation in the present study. Moreover, by the observation in Figures 5 and 8, it is concluded that the backward reaction of Reaction [1] is not significant for the conditions considered in the present study.

### D. Effect of Various Factors on Steel/Flux Reaction: (pct MnO), (pct Fe<sub>2</sub>O), and (pct Na<sub>2</sub>O)

As seen in Figure 3, there are also minor changes of concentrations of MnO, Fe<sub>2</sub>O, and Na<sub>2</sub>O in the molten flux during the reaction with molten steel. It is interesting to note whether the factors varied in the present study also affect the (pct MnO), (pct Fe<sub>2</sub>O), and (pct Na<sub>2</sub>O) in order to extract additional chemical reactions apart from Reaction [1].

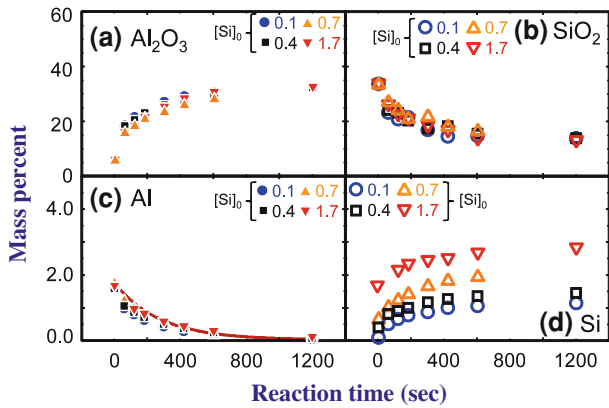


Fig. 8—Effect of [pct Si] on the composition evolution in molten flux (F1) and molten steel (S1, S5, S6, and S7) reacted at 1773 K (1500 °C): (a) (pct Al<sub>2</sub>O<sub>3</sub>), (b) (pct SiO<sub>2</sub>), (c) [pct Al], and (d) [pct Si]. Line in (c) is a calculated [pct Al] using a kinetic equation described in the second article in the present series.<sup>[10]</sup>

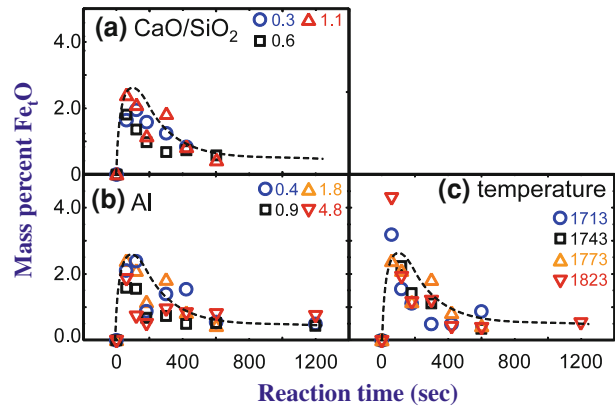


Fig. 10—Evolution of (pct Fe<sub>2</sub>O) in molten flux by chemical reaction between (a) molten flux (F1, F2, and F3) and molten steel (S1) at 1773 K (1500 °C), (b) molten flux (F1) and molten steel (S1, S2, S3, and S4) at 1773 K (1500 °C), and (c) molten flux (F1) and molten steel (S1) at 1713 K to 1823 K (1440 °C to 1550 °C). Dashed lines are to guide the eye.

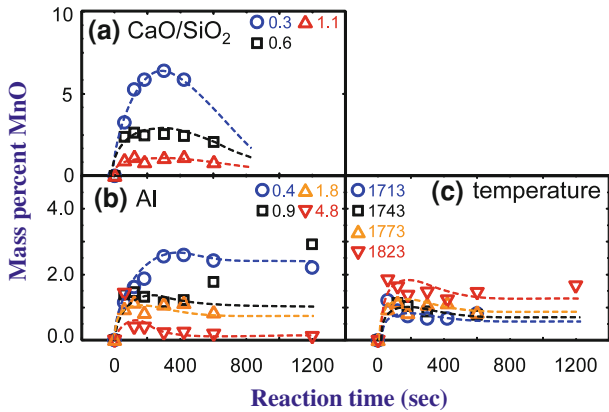


Fig. 9—Evolution of (pct MnO) in molten flux by chemical reaction between (a) molten flux (F1, F2, and F3) and molten steel (S1) at 1773 K (1500 °C), (b) molten flux (F1) and molten steel (S1, S2, S3, and S4) at 1773 K (1500 °C), and (c) molten flux (F1) and molten steel (S1) at 1713 K to 1823 K (1440 °C to 1550 °C). Dashed lines are to guide the eye.

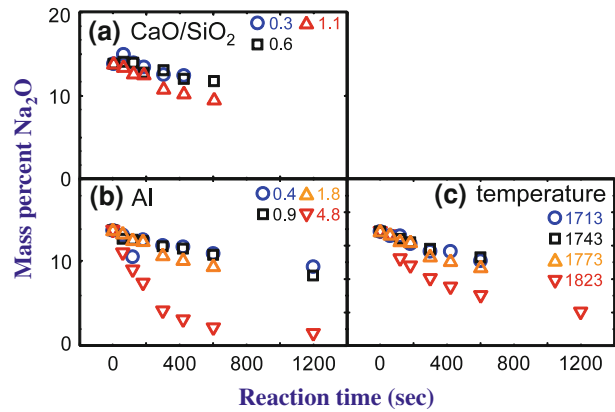
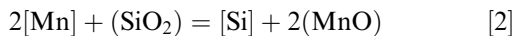


Fig. 11—Evolution of (pct Na<sub>2</sub>O) in molten flux by chemical reaction between (a) molten flux (F1, F2, and F3) and molten steel (S1) at 1773 K (1500 °C), (b) molten flux (F1) and molten steel (S1, S2, S3, and S4) at 1773 K (1500 °C), and (c) molten flux (F1) and molten steel (S1) at 1713 K to 1823 K (1440 °C to 1550 °C).

Shown in Figure 9 is the composition change of MnO in molten flux under different conditions (pct CaO/pct SiO<sub>2</sub>, [pct Al], and temperature). During the reaction between the molten flux and the molten steel, (pct MnO) increased by oxidation of Mn in the molten steel. The increase is more evident when (1) (pct CaO/pct SiO<sub>2</sub>) in molten flux is low, (2) initial [pct Al] is low, and (3) temperature is high. From observation (1), it is thought that the following reaction takes place:



due to abundance of Mn in the liquid steel. And, the reaction is accelerated by decreasing (pct CaO/pct SiO<sub>2</sub>) from observation (1) and increasing temperature from observation (3). However, the oxidized MnO seems to be reduced again by Al from observation (2):



Exhibiting a maximum in (pct MnO) vs time curves implies that Mn in molten steel was rapidly oxidized at the beginning of the reaction, but as (pct MnO) approached at certain level, further oxidation of Mn is prohibited by the presence of Al in the molten steel.

As for (pct Fe<sub>2</sub>O) shown in Figure 10, no meaningful effect of the variables (pct CaO/pct SiO<sub>2</sub>, [pct Al], and temperature) could be observed. However, a definite finding in the present study is that Fe in the molten steel also rapidly oxidized at the beginning of the reaction as Mn did. Then, the Fe<sub>2</sub>O was rapidly reduced. As the decrease of (pct Fe<sub>2</sub>O) seems not to depend on [pct Al] (see Figure 10(b)), it may be postulated that the Fe<sub>2</sub>O was reduced by several elements, not only Al, but also Si and Mn.

Decrease of (pct Na<sub>2</sub>O) is likely to be attributed to the evaporation as gaseous species or reduction by Al in the liquid steel. As shown in Figure 11, the rate of (pct Na<sub>2</sub>O) decrease is high when 1) (pct CaO/pct SiO<sub>2</sub>) = 1.1



**Table II. Effect of Various Factors Affecting Composition Evolution in Molten Flux by Chemical Reactions with Molten Steel**

	(pct Al <sub>2</sub> O <sub>3</sub> )	(pct SiO <sub>2</sub> )	(pct MnO)	(pct Fe <sub>7</sub> O)	(pct Na <sub>2</sub> O)
Temperature	mild	mild	mild	d.j.*	mild
pct CaO/pct SiO <sub>2</sub>	weak	weak	strong	weak	weak
pct Al <sub>2</sub> O <sub>3</sub>	weak	weak	weak	weak	weak
pct Al	strong	strong	strong	weak	strong
pct Si	weak	weak	weak	weak	weak

\*Difficult to judge.

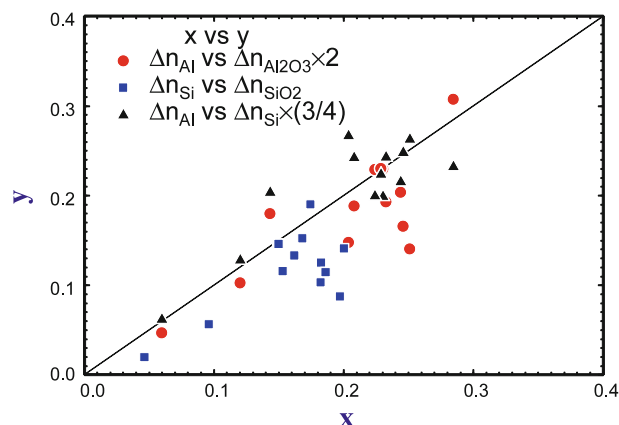
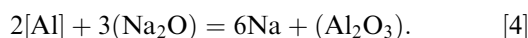


Fig. 12—Calculated mass balance for mass transfer of Al/Al<sub>2</sub>O<sub>3</sub>, mass transfer of Si/SiO<sub>2</sub>, and relative mass change of Al and Si in steels.

compared to 0.3 and 0.6, and 2) [pct Al] = 4.8 compared to 0.4, 0.9, and 1.8. When there is less chance for the Na<sub>2</sub>O to be reduced (CaO/SiO<sub>2</sub> ≤ 0.6 and [pct Al] ≤ 1.8), the rate of (pct Na<sub>2</sub>O) decrease was irrespective of those factors. Under these conditions, the (pct Na<sub>2</sub>O) decrease may be mainly due to evaporation. On the other hand, when (pct CaO/pct SiO<sub>2</sub>) = 1.1 or [pct Al] = 4.8, the Na<sub>2</sub>O is thought to be reduced by Al in the molten steel due to less SiO<sub>2</sub> in the flux or high Al in the steel as



where the reduced Na may be entered into molten steel or may be evaporated into gas phase.

There was no noticeable effect of [pct Si] and (pct Al<sub>2</sub>O<sub>3</sub>) for the (pct MnO), (pct Fe<sub>7</sub>O), and (pct Na<sub>2</sub>O) changes. A summary of the observations in this section is shown in Table II.

### E. General

Simple mass balance calculations were done for mass transfer of Al and Si between molten steel and molten flux and relative mass changes of Al and Si in steel, and the results are shown in Figure 12. As for the mass transfer of Al expressed as  $\Delta n_{\text{Al}}$  vs  $\Delta n_{\text{Al}_2\text{O}_3} \times 2$ , and as for the mass transfer of Si expressed as  $\Delta n_{\text{Si}}$  vs  $\Delta n_{\text{SiO}_2}$ , both should lie on a 1:1 line. Some deviations from the line seem due to the MgO erosion from the refractory

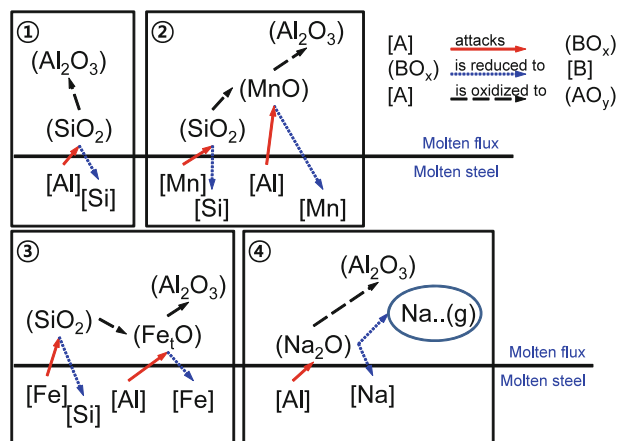


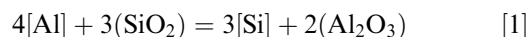
Fig. 13—Schematic representations of major chemical reactions at the interface between molten flux (CaO-SiO<sub>2</sub>-Al<sub>2</sub>O<sub>3</sub>-MgO-Na<sub>2</sub>O-F) and molten steel (Fe-Mn-Al-Si).

and Na<sub>2</sub>O vaporization in the flux side. As for the relative mass change of Al and Si expressed as  $\Delta n_{\text{Al}}$  vs  $\Delta n_{\text{Si}} \times (3/4)$ , which is also supposed to lie on the 1:1 line, some deviations may be due to the role of other elements like Mn and Fe as discussed in this section.

Finally, important reactions between molten steel and molten flux employed in the present study are schematically shown in Figure 13, according to observations discussed above. Although the figure shows only qualitative possible interactions between the molten steel and the molten flux, it is thought to be useful in understanding chemical reactions at a glance. A detailed kinetic analysis utilizing composition evolution and interfacial morphology and a model development to predict Al<sub>2</sub>O<sub>3</sub> accumulation in molten mold flux during continuous casting will be presented in the second article in the present series.<sup>[10]</sup>

## V. CONCLUSIONS

In order to elucidate a reaction mechanism between conventional CaO-SiO<sub>2</sub>-type mold flux and high Mn-high Al steel such as TWIP steel, a series of laboratory-scale experiments were performed in the present study. It was confirmed that the following reaction is the most dominant at the interface between the molten flux and the molten steel:



A number of factors were varied in order to find the major factor which affects the above Reaction [1]. Among those factors varied in the present study ((pct CaO/pct SiO<sub>2</sub>), (pct Al<sub>2</sub>O<sub>3</sub>), [pct Al], temperature, and [pct Si]), [pct Al] was the most dominant factor such that the higher the initial [pct Al], the more the (pct Al<sub>2</sub>O<sub>3</sub>) increased in the molten flux. Increasing temperature slightly promoted the above reaction. The extent of backward reaction of the above reaction seems to be negligible.

Not just the Al, but Mn and Fe were also oxidized, probably competing with Al in reducing SiO<sub>2</sub> due to its high concentrations in the molten steel. However, it was found that the oxidized MnO and Fe<sub>2</sub>O were also reduced by the Al, since the Al is a much stronger oxidizable element. Na<sub>2</sub>O in the molten flux was also found to be reduced by the Al; however, it is not very clear whether Na evaporated or entered into the molten steel.

From the experimentally obtained results in the present study, it is evident that Al<sub>2</sub>O<sub>3</sub> accumulation in the mold flux is very difficult to avoid as long as [pct Al] is high enough to reduce SiO<sub>2</sub> in the mold flux. Changing flux chemistry such as (pct CaO/pct SiO<sub>2</sub>), (pct Al<sub>2</sub>O<sub>3</sub>), and casting temperature would not be effective for suppressing the Al<sub>2</sub>O<sub>3</sub> accumulation in the mold flux.

#### ACKNOWLEDGMENTS

This work was financially supported by POSCO Ltd. through the Steel Innovation Program (Project No. 20118060) to the Graduate Institute of Ferrous Technology, Pohang University of Science and Technology.

#### REFERENCES

1. J. Jin and Y. Lee: *Acta Mater.*, 2012, vol. 60, pp. 1680–88.
2. B. de Cooman, K.-G. Chin, and J. Kim: *New Trends and Developments in Automotive System Engineering*, InTech, Winchester, UK, 2011, pp. 101–28.

3. Y.S. Chun, K. Park, and C.S. Lee: *Scripta Mater.*, 2012, vol. 66, pp. 960–65.
4. K. Park, K.G. Jin, S.H. Han, S.W. Hwang, K. Choi, and C.S. Lee: *Mater. Sci. Eng. A*, 2010, vol. 527, pp. 3651–61.
5. K. Blazek, H. Yin, G. Skoczylas, M. McClymonds, and M. Frazee: *Proc. of 7th European Continuous Casting Conference*, Steel Institute VDEh, Düsseldorf, Germany, 2011, p. Session 9-1.
6. K. Blazek, H. Yin, G. Skoczylas, M. McClymonds, and M. Frazee: *Proc. of AIST 2011*, Association for Iron and Steel Technology, Warrendale, PA, USA, 2011, 1577–86.
7. X. Yu, G.-H. Wen, P. Tang, F.-J. Ma, and H. Wang: *J. Iron Steel Res. Int.*, 2011, vol. 18, pp. 20–25.
8. Q. Wang, S. Qiu, and P. Zhao: *Metall. Mater. Trans. B*, 2012, vol. 43B, pp. 424–30.
9. J.-W. Cho, M.-S. Park, J. Park, K.-H. Moon, and S.-E. Kang: POSCO Ltd., 2012, unpublished research.
10. Y.-B. Kang, M.-S. Kim, S.-W. Lee, J.-W. Cho, M.-S. Park, and H.-G. Lee: *Metall. Mater. Trans. B*, 2012. DOI: [10.1007/s11663-012-9769-5](https://doi.org/10.1007/s11663-012-9769-5).
11. J. Fulton and J. Chipman: *Trans. Metall. Soc. AIME*, 1959, vol. 215, pp. 888–91.
12. E. Turkdogan, P. Grieveson, and J. Beisler: *Trans. Metall. Soc. AIME*, 1963, vol. 227, pp. 1265–74.
13. J. Rawling and J. Elliott: *Trans. Metall. Soc. AIME*, 1965, vol. 233, pp. 1539–45.
14. M. Ashizuka, M. Tokuda, and M. Ohtani: *Tetsu-to-Hagane*, 1968, vol. 54, pp. 1437–46.
15. Y. Kawai, K. Mori, and M. Sakaguchi: *Tetsu-to-Hagane*, 1970, vol. 56, pp. 1447–55.
16. H. Sun, K. Mori, and R. D. Pehlke: *Metall. Trans. B*, 1993, vol. 24B, pp. 113–20.
17. P. Riboud and L. Lucas: *Can. Metall. Q.*, 1981, vol. 20, pp. 199–208.
18. H. Gaye, L. Lucas, M. Olette, and P. Riboud: *Can. Metall. Q.*, 1984, vol. 23, pp. 179–91.
19. H. Ooi, T. Nozaki, and H. Yoshii: *Trans. ISIJ*, 1974, vol. 14, pp. 9–16.
20. B. Ozturk and E.T. Turkdogan: *Met. Sci.*, 1984, vol. 18, pp. 306–09.
21. H. Sun and K. Mori: *ISIJ Int.*, 1996, vol. 36, pp. S34–S37.
22. M.A. Rhamdhani, K.S. Coley, and G.A. Brooks: *Metall. Mater. Trans. B*, 2005, vol. 36B, pp. 219–27.
23. J.W. Robison and R.D. Pehlke: *Metall. Trans.*, 1974, vol. 5, pp. 1041–51.
24. E. Forster and H. Richter: *Arch. Eisenhüttenw.*, 1968, vol. 39, pp. 595–604.
25. H. Gaye and P.V. Riboud: *Metall. Trans. B*, 1977, vol. 8, pp. 409–15.
26. A. Sharan and A. Cramb: *Metall. Mater. Trans. B*, 1995, vol. 26B, pp. 87–94.
27. Y. Chung and A. Cramb: *Philos. Trans. R. Soc. Lond. A*, 1998, vol. 356, pp. 981–93.
28. A. Wu, P.C. Hayes, and H.-G. Lee: *ISIJ Int.*, 1998, vol. 38, pp. 213–19.
29. Y. Chung and A. Cramb: *Metall. Mater. Trans. B*, 2000, vol. 31B, pp. 957–71.
30. D.-J. Kim and J.H. Park: *Metall. Mater. Trans. B*, 2012, vol. 43B, pp. 875–86.